JSTEM

Interaction between Repetitive Lysine and Histidine Peptides and DNA Influenced by Their Pattern and pH of Solution

Yan Hao, Huan Yan, Gaowei Lin and Yanwei Wang*

College of Mathematics and Physics, Wenzhou University, China; 22451026002@stu.wzu.edu.cn(Y.H.), 3476457472@qq.com(H.Y.), 1687358565@qq.com(G.L.)

* Correspondence: wangyw@wzu.edu.cn(Y.W.); Tel.: +86-577-8668-9033; Fax: +86-577-8668-9010

Abstract: DNA is usually compacted by histones, allowing it to fit within the nucleus in cells. The histones are basic proteins mainly consisting of positively charged lysine (K), arginine(R) and histidine(H) residues, binding negatively charged DNA by ionic bonds easily. They maintain protein structure, mediate DNA binding and regulate cellular signaling through their unique chemical properties. In this study, the interaction between repetitive KH polypeptide and DNA was systematically studied by single-molecular magnetic tweezers (MT) and dynamic light scattering (DLS) techniques. We found that DNA condensing force and electrophoretic mobility were modulated by the length of polypeptide chain, the polypeptide sequence pattern and the solution environment. Specifically, more ordered pattern of repetitive KH polypeptides applies significantly stronger DNA condensing force than the one from the disordered polypeptides with the same length. It can be ascribed to its stronger electrostatic interaction with DNA. We also found that the acidic condition (pH = 6.3) promoted condensing force of DNA due to the protonated α-amino group and imidazole side chain of histidine. Our findings provide a molecular insights for design of gene carriers and drug delivery systems.

Keywords: DNA condensation, charge neutralization, magnetic tweezers, repetitive peptides

Received: April 27, 2025
Revised: May 4, 2025
Accepted: May 5, 2025
Published: May 12, 2025

Citation: Hao Y., Yan H., Lin G. and Wang Y. Interaction between Repetitive Lysine and Histidine Peptides and DNA Influenced by Their Pattern and pH of Solution. Journal of STEM 2025, 2(1), 00006. https://doi.org/10.63460/IRVS3852

1. Introduction

As a double helix biomolecule carrying genetic information, deoxyribonucleotide[1] has a phosphate backbone that gives the molecular chain a significant negative charge and a flexible polyanionic character in solution[2]. DNA condensation phenomenon arises from the charge neutralisation effect[3, 4]. When cationic ligands (e.g., ions, proteins, etc.) overcome the repulsive forces between phosphate groups by electrostatic forces, the molecular strands conformationally contract and form a compact structure[5, 6]. This process is not only the physical basis of chromatin assembly and gene expression regulation[7], but also provides a key mechanism for gene delivery technology[8]. By regulating the state of DNA condensation, we can achieve efficient loading and targeted release of therapeutic genes, which is of great value in the field of gene therapy and synthetic biology.

In eukaryotes, dynamic interactions between DNA and histones form the structural basis of epigenetic regulation. It has been resolved the 2.8 Å high-resolution structure of the nucleosome by X-ray crystallography, revealing the precise assembly pattern of DNA wrapped around the histone octamer at a length of ~147 bp, providing a landmark breakthrough in understanding the 3D conformation of the basic unit of chromatin[9]. Allis et al. elucidated the molecular logic of histone post-translational modifications (e.g. acetylation, methylation) affecting gene transcriptional activity through dynamic regulation of chromatin accessibility[10]. It has been revealed that the modification relaxes the chromatin

superhelix structure by neutralizing the positive charge of lysine residues, allowing transcription factors to approach the target DNA sequence[11]. The characteristic force spectral curves of polyarginine-DNA complexes has been measured by MT, which quantitatively revealed the dynamic mechanical features of cationic ligand-DNA binding[12]. Moreover, M. Taipale demonstrated by in vitro reconstitution experiments that specific acetylation of the H4K16 site directly inhibits higher-order folding of chromatin 30 nm fibers and significantly enhances the accessibility of DNA damage repair factors to chromatin-localized structures[13]. These results not only constructed the three-dimensional structural basis of epigenetic regulation, but also provided new molecular perspectives for targeted intervention of abnormal chromatin remodelling in complex diseases such as cancer.

In organisms, the realization of DNA function is highly dependent on interactions with proteins. Histones, the basic units of eukaryotic chromatin[14, 15] are enriched with lysine (K)[16] and histidine (H)[17] to dynamically regulate DNA accessibility through post-translational modifications (e.g. acetylation, methylation)[18, 19]. The positively charged residues of lysine stabilize the DNA phosphoskeleton through electrostatic interaction, whereas the imidazole ring of histidine participates in proton transfer[20, 21] and metal coordination by virtue of its unique acid-base buffering capacity, and both synergistically mediate the dynamic assembly of DNA-protein complexes[22]. It has been shown that KH structural domains are widely present in RNA-binding proteins and are involved in post-transcriptional processing of genes through sequence-specific recognition and conformational regulation, and that their aberrant function is closely related to a variety of genetic diseases[23]. In recent years, the study of synthetic peptides mimicking the function of natural proteins has provided new ideas for resolving DNA-protein interactions[24]. Seeman's DNA nanotechnology builds biocompatible smart nanostructures through the precise self-assembly of DNA-peptide complexes, providing a new paradigm in molecular engineering for biomedical and functional materials development[25]. Pouton et al. investigated the formation mechanism of peptide-DNA complexes and found that the charge density and length of the peptide affect the stability of the complexes[26]. He X. et al. employs single-molecule techniques to elucidate the binding mechanisms and dynamic interactions between cationic short peptides and DNA, providing insights into their structural and functional implications for gene delivery and nanobiotechnology[27]. Xing Y. et al. utilizes single-molecule approaches to dissect the dynamic binding behavior and structural modulation between DNA and repetitive peptides [28]. It has been revealed the regulation mechanism of DNA condensation by multivalent ions[29, 30], cationic polymers[31], pH[32, 33], and so on, there is still a lack of systematic exploration of the dynamic mechanisms of how the sequence design of KH polypeptides affect DNA condensation kinetics, especially at the single-molecule level.

In present study, we employed single-molecule magnetic tweezers (MT) and dynamic light scattering (DLS) techniques to reveal the interaction between repetitive KH polypeptide and DNA, and our study focused on the influence by the length of peptide, sequence pattern of peptide, and pH of solution.

2. Results

2.1 Effect of the chain length of the polypeptides on DNA condensation

In order to investigate the structure-dependent interactions between peptides and DNA, we used both magnetic tweezers (MT) and dynamic light scattering (DLS) techniques. Our experimental results show significant changes in two key interaction parameters: electrophoretic mobility (quantified by zeta potential measurements) and intermolecular critical condensing force.

This study employed magnetic tweezers (MT) to investigate the critical condensing force of λ-DNA condensation induced by K15H15 peptides at varying concentrations (Fig.

1). At 0.5 ng/μL (Fig. a), electrostatic interactions between positively charged lysine residues in the peptide and the negatively charged DNA phosphate backbone partially neutralized DNA charges, reducing inter-DNA repulsion and initiating localized condensation, with a critical force of 8.2 pN. Increasing the peptide concentration to 1 ng/μL (Fig. b) enhanced charge neutralization, significantly suppressing repulsive forces and driving large-scale DNA condensation, as evidenced by a peak critical force of 14.7 pN. However, at 2 ng/μL (Fig. c), excessive peptide adsorption induced DNA surface charge reversal (net positive charge), reintroducing electrostatic repulsion between DNA molecules and reducing the critical force to 2.6 pN. Further increasing concentrations to 3 ng/μL (Fig. d) saturated DNA surface charges, stabilizing condensation behavior in dynamic equilibrium with critical forces plateauing at low levels (4.1 pN). These results demonstrate a non-monotonic trend in critical condensation force—initially increasing, peaking, then decreasing—before stabilizing, highlighting the pivotal role of peptide concentration in regulating DNA condensation dynamics through charge-mediated mechanisms.

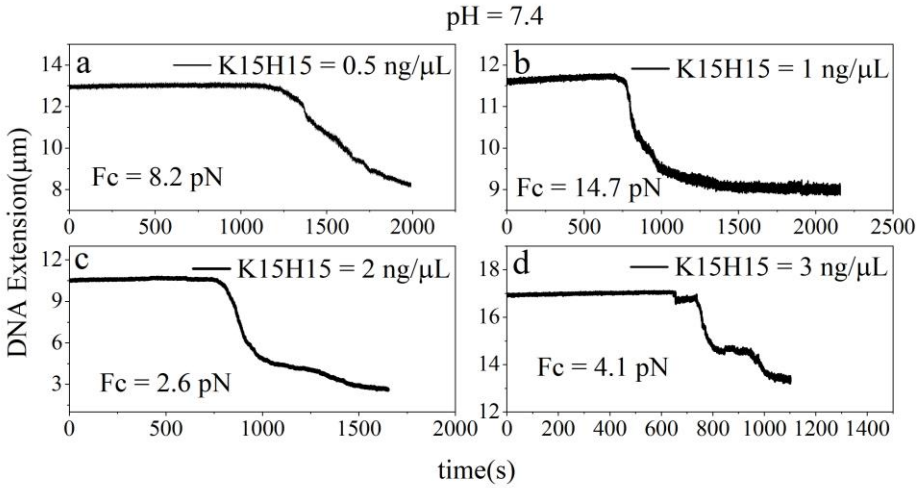

Figure 1. Condensation between K15H15 peptide and DNA in a neutral environment at pH 7.4. a-d present the effects of different concentrations of K15H15 on the DNA condensation, which were 0.5 ng/μL, 1 ng/μL, 2 ng/μL and 3 ng/μL, respectively.

Now we switch to the effect of short chain polypeptides on the condensation of DNA. Similarly, the cohesive behavior of K5H5 DNA was investigated using the MT technique. In the experiment, different concentrations of K5H5 were gradually added to the DNA solution to observe the change of its critical condensation. The results showed that the condensation phenomenon of DNA was gradually enhanced with the increase of K5H5 concentration, and gradually weakened and finally stabilized after reaching the maximum critical condensation peak. The specific data are shown in Fig. 2: as shown in Fig. a, when the concentration of K5H5 was 1 ng/μL, the DNA began to coalesce, and the critical condensation was 3.6 pN; as shown in Fig. b, when the concentration was increased to 2 ng/μL, the critical condensation of DNA reached a peak of 10.1 pN. However, the critical condensation of DNA gradually decreased with the further increase of K5H5 concentration. As shown in Figs. c, d, and e, when the concentration of K5H5 was 3 ng/μL, the critical condensation decreased to 9.9 pN; when the concentration increased to 4 ng/μL, the critical condensation further decreased to 1.3 pN. It can be seen that K5H5 can effectively induce DNA condensation, and its critical condensation trend is similar to that of K15H15.

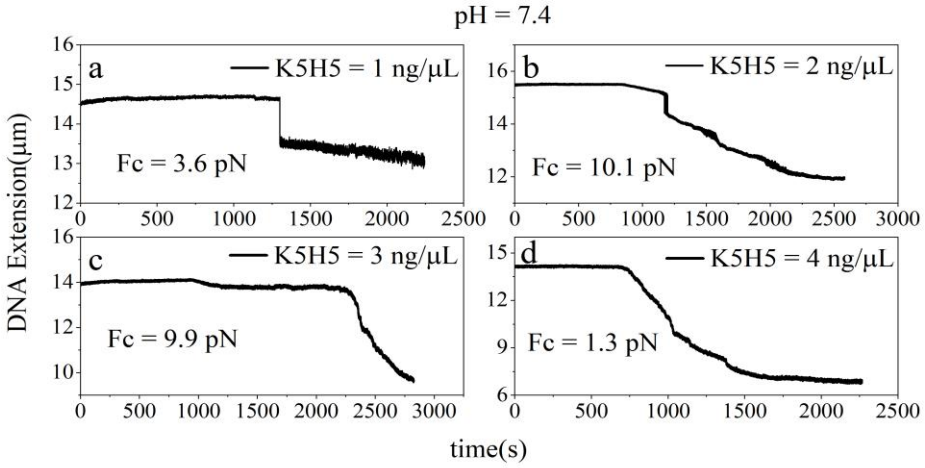

Figure 2. Condensation between K5H5 peptide and DNA under neutral conditions at pH 7.4. a-d demonstrate the effect of different concentrations of K5H5 on the DNA aggregation effect, which were 1 ng/μL, 2 ng/μL, 3 ng/μL, and4 ng/μL, respectively.

In order to further verify this mechanism, we carried out an in-depth study of the electrophoretic mobility of K15H15 and K5H5 with DNA using the DLS technique, and the relevant results are shown in Figure 3. As can be seen from Fig. 3a, the electrophoretic mobility of DNA gradually increased from the initial -2.7 μmcm/Vs as the concentration of K15H15 increased. When the concentration of K15H15 increased to about 0.3 ng/μL, the electrophoretic mobility of DNA reached -0.2 μmcm/Vs; when the concentration was further increased to 0.5 ng/μL, the electrophoretic mobility jumped significantly to 0.8 μmcm/Vs. This change clearly indicated that the DNA underwent the charge reversal phenomenon. In 3b, the electrophoretic mobility of DNA gradually increased from the initial -2.7 μmcm/Vs. When the concentration of K5H5 reached 0.5 ng/μL, the electrophoretic mobility increased to -1.4 μmcm/Vs; as the concentration of K5H5 continued to increase to 3 ng/μL, the electrophoretic mobility tended to be close to 0 μmcm/Vs. This result further confirmed the significant regulation of DNA electrophoretic mobility by K15H15.

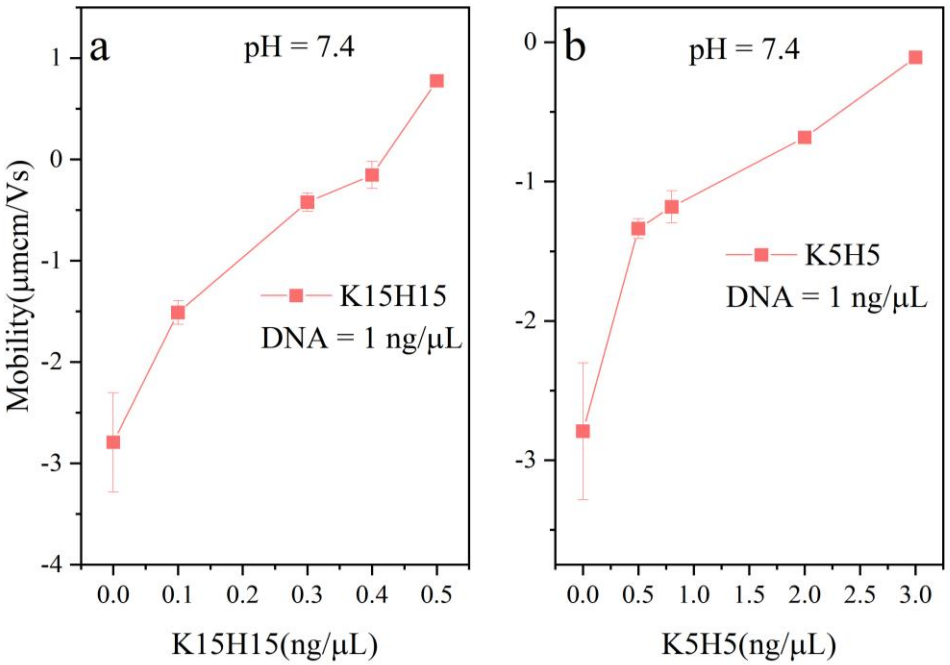

Figure 3. Effect of two peptides, K5H5 and K15H15, on the electrophoretic mobility of DNA in an environment with a pH value of 7.4. a shows the electrophoretic mobility of K15H15 and DNA, the concentrations of K15H15 are 0 ng/μL, 0.1 ng/μL, 0.3 ng/μL, 0.4 ng/μL and 0.5 ng/μL successively. b shows the electrophoretic mobility of K5H5 and DNA,the concentrations of K5H5 are 0 ng/μL, 0.5 ng/μL, 0.8 ng/μL, 2 ng/μL and 3 ng/μL successively.

After analyzing the effects of K15H15 and K5H5 on the condensation of DNA and the electrophoretic migration rate, we found that the interaction between K15H15 and DNA was significantly stronger than that of K5H5 under the same experimental conditions, a conclusion that can be clearly verified by comparing Figures 1 and 2. Further observing the electrophoretic migration rate of DNA, we found that K15H15 was able to induce the occurrence of DNA charge reversal phenomenon at much lower concentration, and this result is visualized in Figure 3. Based on these experimental data, we can clearly conclude that K15H15 exhibits a superior performance than K5H5 in promoting DNA condensation.

2.2 Effect of amino acid sequence on polypeptide-DNA condensation

Firstly, we carried out a systematic study of the cohesive behavior of DNA with the polypeptide $(K3H3)_5$ using the MT technique. In the experiment, the coalescence phenomenon of DNA was observed and analyzed by gradually adding different concentrations of $(K3H3)_5$ to the DNA solution. As shown in Figure 4, when the concentration of $(K3H3)_5$ was as low as 0.5 ng/μL, the DNA molecules began to show a tendency to coalesce, and at this time, the critical condensation was about 1.5 pN. With the increase of the concentration of $(K3H3)_5$, the cohesive effect of DNA was significantly enhanced, and the critical condensation reached a peak value of 11.6 pN when the concentration reached 1.5 ng/μL, which indicated that at this time, the peptide-DNA interaction was most significant. However, when the concentration of $(K3H3)_5$ continued to increase, the critical condensation gradually weakened, a trend similar to the experimental results of K15H15 and K5H5. These results suggest that $(K3H3)_5$ can effectively promote the interaction between DNA molecules and induce DNA condensation in a specific concentration range.

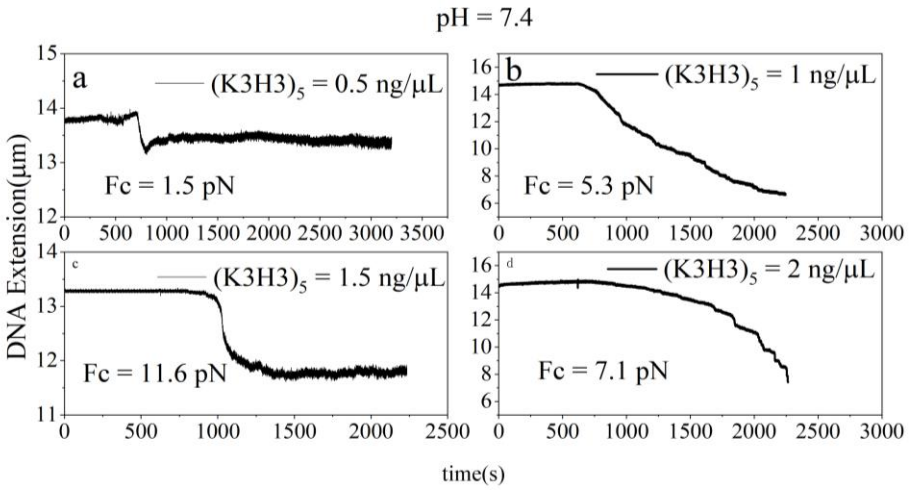

Figure 4. Coalescence between $(K3H3)_5$ polypeptide and DNA molecules occurring at pH 7.4. a-d demonstrate the specific effects of different concentration of $(K3H3)_5$ on the DNA coagulation effect, which are 0.5 ng/μL, 1 ng/μL, 1.5 ng/μL, and 2 ng/μL, respectively.

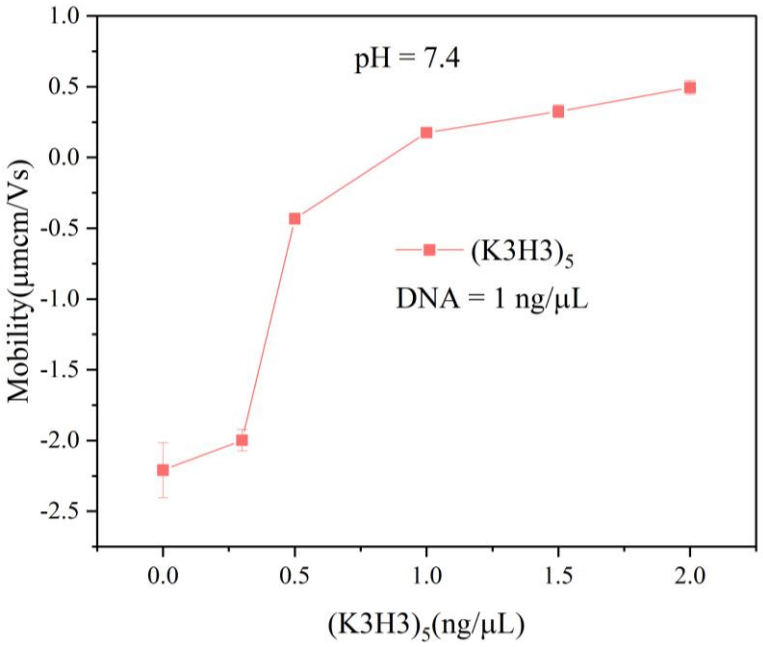

Figure 5. The electrophoretic mobility of $(K3H3)_5$ and DNA under the condition of pH = 7.4,the concentrations of $(K3H3)_5$ are 0 ng/μL, 0.3 ng/μL, 0.5 ng/μL, 1 ng/μL, 1.5 ng/μL and 2 ng/μL successively.

Then, we employed DLS for the measurements to ensure that the concentration of DNA was constant at 1 ng/μL, while the concentration of $(K3H3)_5$ was adjusted to explore its effect on the electrophoretic mobility of DNA. As shown in Figure 5, the electrophoretic mobility of DNA increased from -2.3 μmcm/Vs to -0.4 μmcm/Vs when the concentration of $(K3H3)_5$ reached about 0.5 ng/μL; when the concentration of $(K3H3)_5$ was 1 ng/μL, the electrophoretic mobility of DNA increased to 0.2 μmcm/Vs. This signifies DNA's charge reversal. With these data, we can tentatively suggest that the electrophoretic mobility of DNA molecules showed concentration-dependent changes with $(K3H3)_5$.This change may be related to the interaction between the $(K3H3)_5$ molecules and the DNA molecules,

which may change the surface charge distribution of the DNA molecules, thus affecting their migratory behavior in the electric field.

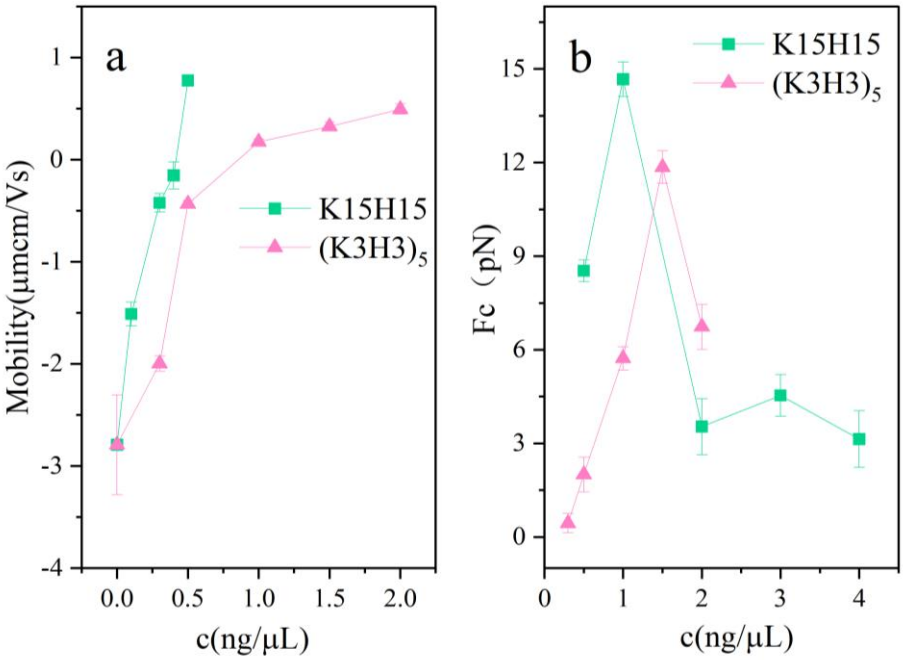

Figure 6. Changes in electrophoretic mobility and critical condensation of two polypeptides, K15H15 and $(K3H3)_5$, upon interaction with DNA at pH 7.4. a shows the electrophoretic mobility profile of K15H15 and $(K3H3)_5$ with DNA, and b shows the change in critical condensation of K15H15 and $(K3H3)_5$ with DNA. The green curve in the figure represents K15H15, while the pink curve represents $(K3H3)_5$.

After analyzing the effects of K15H15 and $(K3H3)_5$ on DNA condensation as well as electrophoretic migration rate, we found that the interaction of K15H15 with DNA was significantly stronger than that of $(K3H3)_5$ under the same experimental condition. As shown in Fig. 6a, we observed a significant charge reversal of DNA when the concentration of K15H15 reached 0.5 ng/μL phenomenon. Similarly, at a concentration of $(K3H3)_5$ of 1 ng/μL, the charge reversal phenomenon of DNA was also clearly observed. Further examining Figure 6b, we can find that at a concentration of 0.5 ng/μL, K15H15 caused DNA coagulation with a critical condensation of 8.2 pN, whereas under the same conditions, $(K3H3)_5$ also caused coagulation at a concentration of 0.5 ng/μL, but its critical condensation was only 1.5 pN. In addition, at a concentration of 1 ng/μL, the condensation of K15H15 had increased to 14.7 pN. condensation had increased to 14.7 pN, whereas the critical condensation of $(K3H3)_5$ was only 5.3 pN. At a concentration of 2 ng/μL, the critical condensation of K15H15 with DNA was significantly higher than that of $(K3H3)_5$, and the increase in critical condensation of K15H15 showed a more significant phase jump, compared to the slower response of $(K3H3)_5$, which indicated that the superiority of K15H15 in DNA condensation.

2.3 Effect of pH on polypeptide and DNA condensation

Lysine and histidine, amino acids with ionizable side chains, exhibit pH-dependent charge states that govern their biological and functional roles[34]. These properties are exploited in specific pH contexts: at pH 6.3 (mimicking endosomal conditions), histidine's protonation triggers nanoparticle escape or payload release during gene delivery[35], while pH 7.4 (physiological blood/tissue conditions) tests biocompatibility and protein behavior. At pH 8.4, simulating alkaline environments like the small intestine or industrial settings,

lysine's reduced charge and histidine's deprotonation influence solubility and enzymatic activity. Together, their pH-sensitive behaviors enable tailored applications in biochemistry, drug delivery, and biomaterial design.

We used the MT technique to adjust the solution pH to 6.3, followed by the addition of different concentrations of K15H15 to the DNA. As shown in Fig. 7, under the condition of pH = 6.3, when the concentration of K15H15 was only 0.5 ng/μL, it could trigger the significant condensation of DNA, and its critical condensation reached 8.4 pN, which indicated that K15H15 exhibited a strong DNA-binding ability at a low concentration. However, as the concentration of K15H15 was increased to 1 ng/μL, the critical condensation of K15H15 with DNA decreased to 2.9 pN, suggesting that there exists an optimal concentration range for the interaction between K15H15 and DNA, beyond which the cohesive effect may be weakened due to the charge reversal or spatial site-blocking effect.

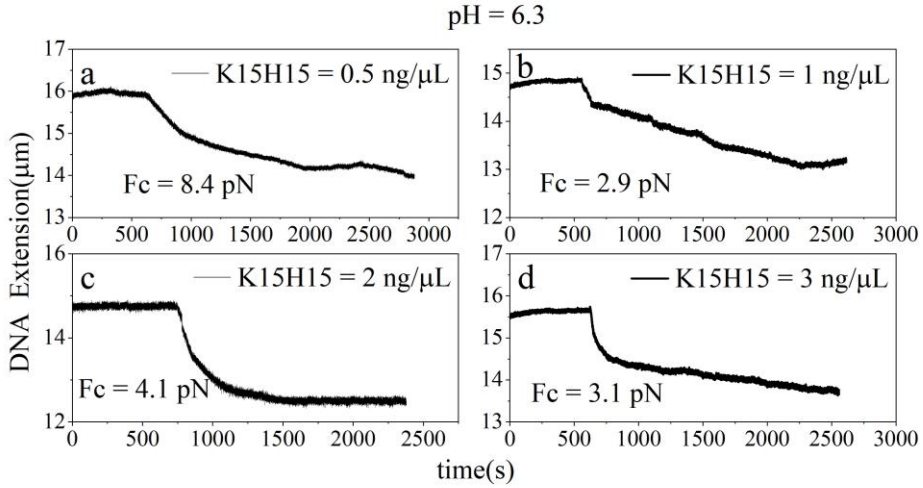

Figure 7. Coagulation of K15H15 with DNA at pH 6.3. a-d show the effect of different concentrations of K15H15 on the DNA coagulation effect, which were 0.5 ng/μL, 1 ng/μL, 2 ng/μL and 3 ng/μL, respectively.

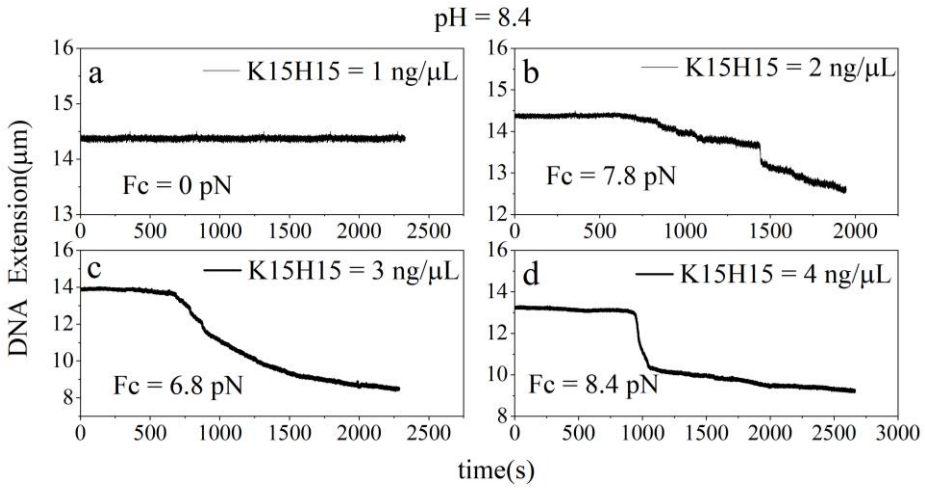

Figure 8. Condensation between K15H15 peptide and DNA molecules in a specific environment at pH 8.4. a-d present the effects of different concentrations of K15H15 on the DNA coagulation effect, which were 1 ng/μL, 2 ng/μL, 3 ng/μL, and 4 ng/μL, respectively.

To further study the effect of pH on the interaction of K15H15 with DNA, we adjusted the solution pH to 8.4 and performed the same experiment. As shown in Figure 8, the

coagulation behavior of K15H15 showed significant differences at pH = 8.4. When the concentration of K15H15 was lower than 2 ng/μL, the DNA did not show significant coagulation; however, when the concentration reached 4 ng/μL, the coagulation effect of DNA reached a peak with a critical coagulation force of 8.4 pN. This result suggests that in an alkaline environment, a higher concentration of K15H15 is required to induce DNA coagulation, which further confirms that the pH has a peptide-nucleic acid interaction of the significant effect of pH on peptide-nucleic acid interactions.

To verify the above mechanism, we investigated the interaction of K15H15 with DNA under different pH conditions using DLS technique (Figure 9). In an acidic environment at pH = 6.3, the electrophoretic mobility of DNA increased from -2.7 μmcm/Vs to -1.4 μmcm/Vs when the concentration of K15H15 reached 0.1 ng/μL; when the concentration was increased to 0.8 ng/μL, the mobility turned to a positive value (0.3 μmcm/Vs), indicating that the DNA underwent charge reversal (Fig. a). In contrast, in an alkaline environment at pH = 8.4, DNA remained significantly negatively charged even at a K15H15 concentration of 2 ng/μL (Fig. b). This phenomenon further confirms that K15H15 interacts more strongly with DNA in acidic environments, and the concentration of K15H15 required for charge reversal is significantly lower.

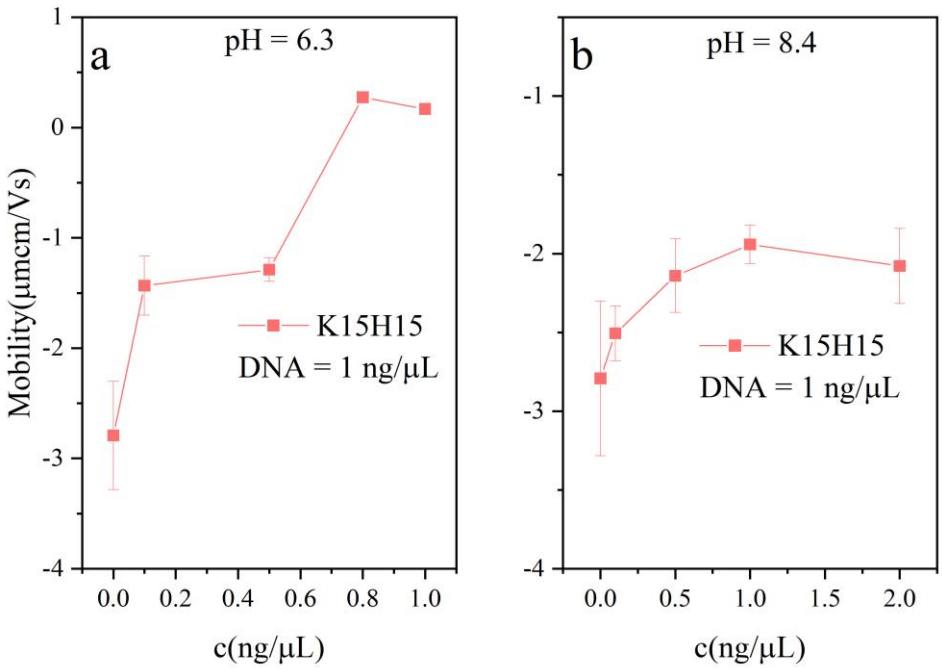

Figure 9. Electrophoretic mobility of K15H15 with DNA under different pH conditions. a reflects the electrophoretic mobility of K15H15 with DNA in a solution environment of pH = 6.3, the concentrations of K15H15 are 0 ng/μL, 0.1 ng/μL, 0.5 ng/μL, 0.8 ng/μL, and 1 ng/μL successively. b demonstrates the electrophoretic mobility of K15H15 with DNA in a solution environment of pH = 8.4, the concentrations of K15H15 are 0 ng/μL, 0.1 ng/μL, 0.5 ng/μL, 1 ng/μL, and 2 ng/μL successively.

When the pH of the solution is lower than 7.0, i.e., when it is in an acidic environment, the cohesive interaction between K15H15 and DNA will show more significant. This phenomenon suggests that condensation is more likely to occur under acidic conditions, while condensation is relatively weak when the pH is greater than 7.0, i.e., in an alkaline environment.

3. Discussion and Conclusions

In present study, the interactions of K15H15, K5H5, and $(K3H3)_5$ with DNA were intensively investigated mainly by MT and DLS techniques, and the cohesive behaviors of the peptides with DNA were modulated by varying the chain lengths and sequences of the peptides and the pH of the solution, and the following conclusions were drawn:

1. K15H15 was significantly more effective than K5H5. By DLS technique, K15H15 induced DNA charge reversal at 0.5 ng/μL, whereas K5H5 required 3 ng/μL for electrophoretic mobility to be close to zero.The MT experiments further demonstrated that K15H15 induced DNA condensation at a peak of 1 ng/μL resulted in peak DNA condensation (14.7 pN), while K5H5 required 2 ng/μL to reach peak condensation (10.1 pN). The results showed that K15H15 was superior to K5H5 in terms of both charge reversal and condensation strength. Combined with the structural analysis (shown in Fig. 10), the chain length of K15H15 was significantly longer than that of K5H5 and it carried a greater number of positive charges, thus it was able to neutralize the negative charges of the DNA more efficiently and enhance the electrostatic interactions with the DNA. In contrast, K5H5 has a relatively weak binding ability to DNA due to its shorter chain length and fewer positive charges. Based on the above results, we conclude that under the same conditions, the longer the chain length of the peptide, the more significant its cohesive effect with DNA. This finding provides an important theoretical basis for the study of peptide-nucleic acid interactions and points out the optimization direction for the design of peptide-based gene delivery systems.

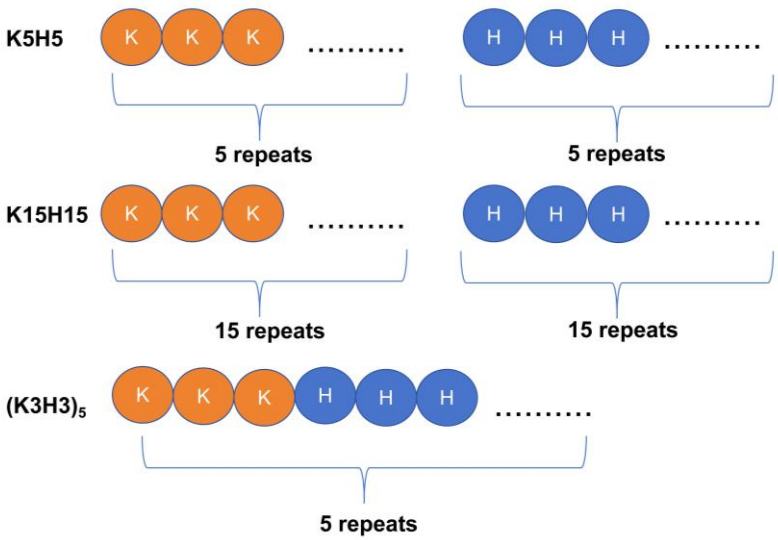

Figure 10. Schematic diagram of the structure of K15H15 and $(K3H3)_5$.

2. K15H15 had a significantly better coagulation effect than $(K3H3)_5$. Using the DLS technique, we found that K15H15 induced DNA charge reversal at a concentration of 0.5 ng/μL, whereas $(K3H3)_5$ required 1 ng/μL to achieve a similar effect. mt experiments further showed that K15H15 caused peak DNA condensation at 1 ng/ μ L (14.7 pN), whereas $(K3H3)_5$ required 1.5 ng/μL to achieve peak condensation (11.6 pN). Combined with the structural analysis (shown in Fig. 10), the disordered peptides were able to form a more stable interaction interface, which significantly enhanced their binding affinity with DNA, whereas the ordered peptides might have a weaker binding affinity with DNA due to the spatial site-barrier effect and dispersed nature of charge distribution. Based on this, we conclude that for the same polypeptide, the order of its arrangement has an important effect on DNA condensation. Specifically, under the condition of the

same chain length, the disordered polypeptide has stronger DNA binding ability than the ordered polypeptide.

3. Acidic conditions induce more significant peptide-DNA condensation than alkaline conditions. Measured by DLS and MT techniques, we found that under acidic conditions (pH = 6.3), K15H15 induced DNA charge reversal at 0.8 ng/μL with significant condensation, and the maximum critical condensation was 8.4 pN, respectively. under neutral conditions (pH = 7.4), K15H15 peaked the DNA condensation at 1 ng/μL, with condensation of 14.7 pN. whereas under alkaline conditions (pH = 8.4), DNA coagulation was weaker, with K15H15 reaching 4 ng/μL to peak coagulation, with a critical coagulation of 8.4 pN. Through structural analyses, the lower concentration of hydroxide ions (OH^-) in the solution at pH = 6.3 and the lower concentration of hydrogen ions (H^+) required to neutralize the DNA requires a relatively greater number of hydrogen ions (H^+), resulting in a tightening of the DNA structure, whereas at pH = 8.4, the concentration of hydroxide ions is higher, and the number of hydrogen ions required to neutralize the DNA correspondingly decreases, resulting in a stretching of the DNA structure. Based on this, we conclude that K15H15 and K5H5 interact more strongly with DNA in acidic environments, which results in lower concentrations required for DNA charge reversal and more significant condensation effects. This phenomenon is mainly attributed to the fact that histidine residues in peptide assemblies in acidic environments are more protonated and carry more positive charges, which enhances the electrostatic interactions with the negatively charged phosphate groups of DNA.

4. Materials and Methods

4.1 Materials

In this experiment, the double-stranded λ-DNA (48,502 bp in length) used for MT and DLS experiments was purchased from New England Biolabs. Ultrapure water produced by the Milli-Q system was employed, and Tris(hydroxymethyl aminomethane), 10 mM Tris-HCl was utilized as the experimental buffer at concentrations of 10 mM and 1 mM, respectively. For the MT experiments, a phosphate-buffered saline (PBS) containing 10 mmol/L phosphate was prepared, with its stock solution being 1×TE buffer. Additionally, lysine-histidine (Lys-His) repeat sequence polypeptides were procured from Jiangsu Jitai Peptide Biotechnology Co., Ltd. (Suzhou, China) in lyophilized powder form. The peptides used included K5H5, K15H15, and $(K3H3)_5$, with amino acid sequences corresponding to KKKKKHHHHH, KKKKKKKKKKKKKKK-HHHHHHHH-HHHHHHH and KKKHHH-KKKHHH
-KKKHHH-KKKHHH-KKKHHH, respectively.

4.2 Dynamic light scattering (DLS)

Dynamic Light Scattering (DLS)[36] is a technique that employs a laser light source to irradiate a sample and measures the intensity and distribution of scattered light to obtain information about particle size. This method is widely applied in biophysics. The working principle of DLS is based on light scattering phenomena: a laser beam illuminates the sample, generating scattered light, and the fluctuations in scattered light intensity and frequency over time are detected to analyze the size distribution and surface charge characteristics of the sample. The Materials and Methods should be described with sufficient details to allow others to replicate and build on the published results. Please note that the publication of your manuscript implicates that you must make all materials, data, computer code, and protocols associated with the publication available to readers. Please dis-

close at the submission stage any restrictions on the availability of materials or information. New methods and protocols should be described in detail while well-established methods can be briefly described and appropriately cited.

DLS can accurately measure the size and distribution of submicron-sized particles in solutions or suspensions, analyze hydrodynamic properties of polymer solutions, and determine the Zeta potential of complexes in solution. Additionally, it is used to study protein folding states, nanoparticle stability, and the stability of emulsions or suspensions. In the experiment, 1 mL of the test sample was placed into a DTS1070 sample tank to measure its electrophoretic mobility.

4.3 Magnetic tweezers (MT)

Magnetic Tweezers (MT)[37] is a high-precision experimental system primarily comprising core components such as an inverted microscope, a sample microchamber, a magnet assembly, a micropipette, a manual manipulation stage, a CCD imaging system, and computerized analysis software. During experiments, the sample microchamber is securely mounted on the platform of the inverted microscope. The micropipette precisely regulates fluid flow rate and volume to maintain sample stability throughout the procedure. The magnet assembly can be laterally displaced during operation, enabling experimenters to apply finely controlled forces to DNA molecules for precise manipulations.

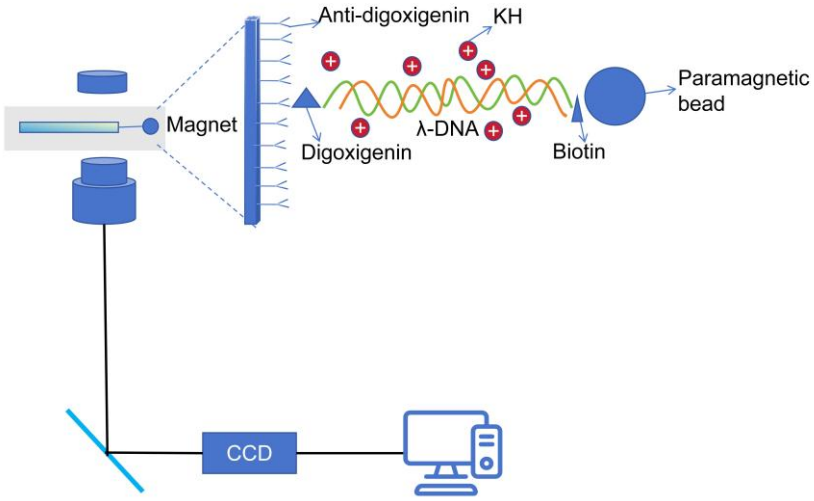

Figure 13. Schematic Diagram of the Structure of the Magnetic Tweezers Device.

The diameter of a DNA molecule is only 2 nm. To effectively manipulate it under an optical microscope, "handles" must be attached to both ends. As shown in Figures 13, the experimental procedure involves the following steps: First, the sidewalls of the cover glass are coated with anti-digoxigenin to enable effective binding between digoxigenin and the sidewalls. Next, magnetic beads are functionalized with streptavidin and mixed with a single-stranded end of the DNA molecule labeled with biotin, forming a DNA-bead hybrid solution. Finally, this solution is introduced into the sample chamber, allowing the DNA to anchor to the anti-digoxigenin-coated sidewalls. By applying an external magnetic field to move the magnetic beads, the "handles" can be controlled to manipulate the DNA molecule.

Author Contributions: Conceptualization, Y.W.; methodology, Y.W.; validation, Y.H.; formal analysis, Y.W. and Y.H.; investigation, H.Y., G.L. and Y.H.; resources, Y.W.; data curation, Y.W. and Y.H.; writing—original draft preparation, Y.H.; writing—review and editing, Y.W.; supervision, Y.W.; project administration, Y.W.; funding acquisition, Y.W. All authors have read **Funding:** This

research was funded by the National Natural Science Foundation of China (12074289,11574232), Natural Science Foundation of Zhejiang Province (LY23A040002) and Wenzhou Municipal Scientific Research Program (L20240004).

Data Availability Statement: Not applicable.

Conflicts of Interest: The authors declare no conflicts of interest.

References

1. Doudna, J.A. and E. Charpentier, *The new frontier of genome engineering with CRISPR-Cas9.* Science (American Association for the Advancement of Science), 2014. **346**(6213): p. 1077-1077.
2. *DNA Structure and Function*. 2012.
3. Manning, G.S., *The molecular theory of polyelectrolyte solutions with applications to the electrostatic properties of polynucleotides.* Quarterly reviews of biophysics, 1978. **11**(2): p. 179-246.
4. Oo, D., et al., *DNA folding by positively charged condensing agents.* Biophysical journal, 2022. **121**(3): p. 211a-211a.
5. Miguel, M.G., et al., *DNA–cationic amphiphile interactions.* Colloids and surfaces. A, Physicochemical and engineering aspects, 2003. **228**(1): p. 43-55.
6. Wang, Y., et al., *DNA condensations on mica surfaces induced collaboratively by alcohol and hexammine cobalt.* Colloids and surfaces, B, Biointerfaces, 2011. **83**(1): p. 61-68.
7. Rangarajan, P.N. and G. Padmanaban, *Gene therapy: Principles, practice, problems and prospects.* Current science (Bangalore), 1996. **71**(5): p. 360-368.
8. Yin, H., et al., *Non-viral vectors for gene-based therapy.* Nature reviews. Genetics, 2014. **15**(8): p. 541-555.
9. Luger, K., et al., *Crystal structure of the nucleosome core particle at 2.8 Å resolution.* Nature (London), 1997. **389**(6648): p. 251-260.
10. Allis, C.D. and T. Jenuwein, *The molecular hallmarks of epigenetic control.* Nature reviews. Genetics, 2016. **17**(8): p. 487.
11. Struhl and K., *Histone acetylation and transcriptional regulatorymechanisms.* Genes Dev, 1998. **12**(5): p. 599-606.
12. Kong Lingxuan, Wang Yanwei, and Yang Guangcan, *Study on the influence of different kinds of ions on DNA condensation. Journal of Qilu University of Technology*, 2022. **36**(5): p. 62-67.
13. Taipale, M., et al., *hMOF Histone Acetyltransferase Is Required for Histone H4 Lysine 16 Acetylation in Mammalian Cells.* Molecular & Cellular Biology, 2005. **25**(15): p. 6798-810.
14. Brosnan, M.E. and J.T. Brosnan, *Histidine Metabolism and Function.* The Journal of nutrition, 2020. **150**(Suppl 1): p. 2570S-2575S.
15. Bonner, H.J., *Histone, a suppressor of chromosomal RNA synthesis.* Proceedings of the National Academy of Sciences, 1962. **48**(7): p. 1216-1222.
16. Schmitz-Schug, I., U. Kulozik, and P. Foerst, *Reaction Kinetics of Lysine Loss in a Model Dairy Formulation as Related to the Physical State.* Food and bioprocess technology, 2014. **7**(3): p. 877-886.
17. Liao, S.M., et al., *The multiple roles of histidine in protein interactions.* Chemistry Central Journal, 2013. **7**(1): p. 1-12.
18. Shi, X., et al., *ING2 PHD domain links histone H3 lysine 4 methylation to active gene repression.* Nature, 2006. **442**(7098): p. 96-99.
19. Uchida, K., *Histidine and lysine as targets of oxidative modification.* Amino Acids, 2003. **25**(3-4): p. 249-257.
20. R., et al., *N–H···N Hydrogen Bonds Involving Histidine Imidazole Nitrogen Atoms: A New Structural Role for Histidine Residues in Proteins.* Biochemistry, 2016. **55**(27).
21. Martínez, A., *Evidence for a functionally important histidine residue in human tyrosine hydroxylase.* Amino Acids, 1995. **9**(3): p. 285-92.

22. Watson, M., et al., *A DNA condensation code for linker histones.* Proceedings of the National Academy of Sciences - PNAS, 2024. **121**(33): p. e2409167121.
23. Nicastro, G., I.A. Taylor, and A. Ramos, *KH–RNA interactions: back in the groove.* Current opinion in structural biology, 2015. **30**: p. 63-70.
24. Quazi, M.Z. and N. Park, *DNA Hydrogel-Based Nanocomplexes with Cancer-Targeted Delivery and Light-Triggered Peptide Drug Release for Cancer-Specific Therapeutics.* Biomacromolecules, 2023. **24**(5): p. 2127-2132.
25. Seeman, N.C., *DNA in a material world.* Nature (London), 2003. **421**(6921): p. 427-431.
26. Pouton, C.W. and L.W. Seymour, *Key issues in non-viral gene delivery.* Advanced drug delivery reviews, 2001. **46**(1): p. 187-203.
27. He, X., et al., *Single molecular investigation of the interactions between cati-onic short peptides and DNA.* Journal of STEM, 2024. **1**: p. 1-00005.
28. Xing, Y., et al., *Single Molecular Study of interaction between DNA and repet-itive peptides.* Journal of STEM, 2024. **1**: p. 1-00003.
29. Bloomfield, V.A., *DNA condensation by multivalent cations.* BIOPOLYM, 1997. **44**(3): p. 269-282.
30. Qiu, S., et al., *The suppression and promotion of DNA charge inversion by mixing counterions.* Soft matter, 2015. **11**(20): p. 4099-4105.
31. Tang, M.X. and F.C. Szoka, *The influence of polymer structure on the interactions of cationic polymers with DNA and morphology of the resulting complexes.* Gene therapy, 1997. **4**(8): p. 823-832.
32. Ma, F., Y. Wang, and G. Yang, *The modulation of chitosan-DNA interaction by concentration and pH in solution.* Polymers, 2019. **11**(4): p. 646.
33. Li, N., et al., *Demonstration of pH-controlled DNA-surfactant manipulation for biomolecules.* RSC advances, 2021. **11**(25): p. 1599-1515.
34. Tu, Z., et al., *The pH sensitivity of histidine-containing lytic peptides.* Journal of Peptide Science An Official Publication of the European Peptide Society, 2010. **15**(11): p. 790-795.
35. Kang, Y., et al., *pH and glutathione dual-triggered supramolecular assemblies as synergistic and controlled drug release carriers.* Polymer Chemistry, 2017: p. 10.1039.C7PY01644A.
36. Ben Yahia, A., et al., *Structure-Elasticity Relationships in Hybrid-Carrageenan Hydrogels Studied by Image Dynamic Light Scattering, Ultra-Small-Angle Light Scattering and Dynamic Rheometry.* Materials, 2024. **17**(17): p. 4331.
37. Yan, J., D. Skoko, and J.F. Marko, *Near-field-magnetic-tweezer manipulation of single DNA molecules.* Physical review. E, Statistical, nonlinear, and soft matter physics, 2004. **70**(1 Pt 1): p. 011905-011905.